Instructions for use

Green Chemistry

ARTICLE

Curdlan Acetate Fibres with Low Degrees of Substitution Fabricated via Continuous Process of Chemical Modification and Wet Spinning Using Ionic Liquid

Shiori Suzuki [§], Azusa Togo, Satoshi Kimura, and Tadahisa Iwata*

Polysaccharide esters with a low degree of substitution (DS) are expected to be biomass-derived biodegradable plastics with tunable properties that will replace conventional petroleum-derived plastics. However, they have difficulties in moulding and the complex multistep synthesis aimed at controlling their DS, thereby limiting their application as plastics. In this study, we demonstrate a continuous process of homogeneous acetylation of curdlan (β-1,3-glucan) and direct wet spinning of the reactant solution by consistently using an ionic liquid, and for the first time, achieve both facile and green synthesis and fabrication of curdlan acetates into fibres with a low DS ranging from 0.1–1.0. The partial acetylation of curdlan improved the thermal stability and fiber properties in both the dry and wet states: thermal degradation temperature ($T_{d-5\%}$) from 293 to 342 °C, Young's modulus (dry) from 2.9 to 4.0 GPa, and tenacity (wet) from 0.34 to 2.8 cN tex^{-1}. Originally, a regenerated curdlan fibre was ductile, with a high water absorbency of 85 wt.%, causing a considerable decrease of the wet tenacity. In contrast, curdlan acetate fibres stiffened, and the water absorbency was suppressed to 15 wt.% at DS = 0.8 owing to the substitution of the C4-OH group (which originally contributed to the incorporation of water into the curdlan molecules). Consequently, the wet-to-dry tenacity ratio of the curdlan acetate fibres significantly improved from 0.03 to 0.5. Such enhanced properties were attributed by acetylation with DS exceeding 0.4 to the change in the crystalline structure due to preventing the formation of hydrogen bonding via the C2-OH group (which stabilised the original triple helical structure).

Introduction

Currently, there is a critical demand for plastics to be replaced with biomass-derived plastics with biodegradability to address the severe environmental problems, such as global warming [1, 2] and land- and marine-pollution, [3] caused by petroleum-derived recalcitrant plastics.[4]

Polysaccharides, produced by plants and microorganisms, are valuable biomass resources with remarkable biodegradability and a variety of structures and properties depending on their constituent monosaccharides and linkage styles. This diversity of polysaccharides and their potential tuneable properties via chemical modification, such as acylation, can contribute to expanding the range of the performance and function of biomass-based materials. However, previous studies on polysaccharides for material applications have been limited to common cellulose and starch, and the potential of other polysaccharides and ester derivatives has not been sufficiently explored.

The final properties of polysaccharide esters depend on the type of backbone structure [5, 6] and ester group,[7, 8] as well as the

degree of substitution (DS).[9-11] The aim of new developments in this field is to understand the relationship between the structure and properties of polysaccharide esters with various DS to meet the desired properties toward a wide range of application. Generally, as the DS increases, the properties derived from the ester group, such as thermoplasticity, solubility, and hydrophobicity, are more strongly reflected, but the inherent biodegradability decreases.[12-14] To address this trade-off, low-substituted polysaccharide esters are preferable. However, they have difficulties in moulding as plastics and the complicated multistep synthetic protocol required to control their DS. In fact, cellulose acetates with DS below 2.2 are not commercialised even though it is the most common biomass plastic, and only a few studies on their fabrication and property evaluation have been published.[10, 11]

Recently, studies on the application of ionic liquids (ILs) in polysaccharide chemistry have attracted significant interest, and have covered all process steps from dissolution [15, 16] and acylation [17-20] of polysaccharides to recycling the used ILs by evaporation of the precipitant agents.[21, 22] When aiming for the production of polysaccharide esters, ILs allow for a green, homogeneous, and fast one-step reaction with easy control of the DS,[17, 19] which does not require corrosive acyl reagents (e.g., acyl halide and acid anhydride) and additional catalyst because ILs act as the solvent and catalyst. Moreover, ILs exhibit great potential for processing insoluble and non-thermal meltable polysaccharides into value-added, shaped products such as

Laboratory of Science of Polymeric Materials, Department of Biomaterial Sciences, Graduate School of Agricultural and Life Sciences, The University of Tokyo, 1-1-1 Yayoi, Bunkyo-ku, Tokyo 113-8657, Japan.
§ Now at Laboratory of Wood Chemistry, Division of Fundamental Agriscience Research, Research Faculty of Agriculture, Hokkaido University, Kita 9, Nishi 9, Kita-ku, Sapporo, Hokkaido 060-8589, Japan.

fibres [23] and films,[24] providing a safe, simple, and green moulding process compared to the existing viscose and lyocell processes that involve the use of toxic reagents and additives.[25]

To be noted again, the insufficient solubility and thermal meltability of polysaccharide esters with low DS have strictly limited their industrial utilisation. In precise, they can be chemically synthesised but cannot be subjected to moulding in solution/bulk and analysing their material properties in detail. Hence, we hypothesised that the difficulty in moulding could be settled by a continuous process of (1) homogeneous acylation of polysaccharides to an arbitrary DS using an IL as a solvent and catalyst and (2) direct fabrication of the reaction solution with the IL-derived specific viscoelasticity into fibres (or films) via highly drawing and coagulating in the poor solvent, such as water. Furthermore, the resultant well-oriented fibres are suitable for the analysis of the changes in the structures and properties with various DS.

In this study, a linear β-1,3-glucan (curdlan)[26] was targeted, which is a bacterial polysaccharide with a unique triple helical structure [27-29] and the associated characteristic properties, [30, 31] in contrast to a historically well-investigated β-1,4-glucan (cellulose). Such unprecedented elucidation of curdlan and the low-substituted esters derivatives can provide new findings of the effects of not only the DS but also the backbone structure of polysaccharides on the material properties. Importantly, curdlan dissolves in dilute alkaline solutions and dimethyl sulfoxide (DMSO), but these solvents are difficult to recycle and lack of appropriate viscoelasticity for dry-jet wet spinning. Thus, a continuous process for synthesis and dry-jet wet spinning using an IL, 1-ethyl-3-methyl-imidazolium acetate ([Emim][OAc]) as the catalyst and dual solvent, was developed, and the facile and green preparation of low-substituted curdlan acetate fibres with enhanced properties was achieved. The comprehensive analysis of physico-chemical, thermal, and mechanical properties and crystalline and molecular chain structures revealed the insights on the correlation between the structure and fibre properties of curdlan and curdlan acetates with low DS, which could contribute to the design and production of a variety of polysaccharide-based materials with the desired properties depending on their application.
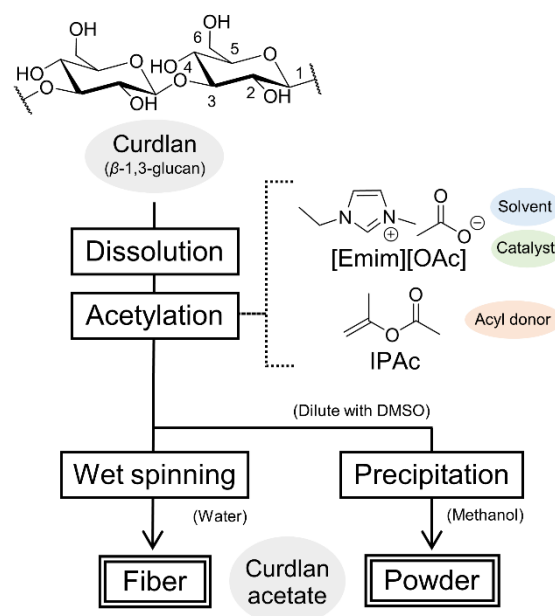
Experimental section

Materials

1-Ethyl-3-methylimidazolium acetate ([Emim][OAc], >95%) was purchased from Nippon Nyukazai Co., Ltd. (Tokyo, Japan) and used without further purification. Biochemical grade curdlan was purchased from Takeda Pharmaceutical Co., Ltd. (Tokyo, Japan). It was repeatedly washed with distilled water and freeze-dried for more than 2 days. The purified curdlan was further dried in a vacuum at 70 °C until a constant weight was obtained before use. Isopropenyl acetate (IPAc >98%), trifluoroacetic acid anhydride (TFAA, >98%), and propionic acid (>99%) were purchased from Tokyo Chemical Industry Co., Ltd. (Tokyo, Japan). Dimethyl sulfoxide (DMSO, >99%) was purchased from FUJIFILM Wako Pure Chemicals Co., Tokyo,

Japan). Other chemicals were commercially available and used as received unless otherwise stated.

Acetylation of curdlan and successive wet spinning

Curdlan was acetylated using [Emim][OAc] and IPAc, and subsequently fabricated into a fibre (or powder), as depicted in Scheme 1. Purified curdlan (9.0 g) in [Emim][OAc] (100 g) was vacuum dried at 80 °C to remove moisture, and its complete dissolution was observed in less than 2 h. IPAc (0−3.0 eq./AGU) was added to the solution under a N_2 atmosphere and stirred for 2 h at 80 °C. The resultant solution was transferred to a stainless-steel barrel equipped with a one-hole spinneret with a capillary diameter of 1.0 mm and a length-to-diameter ratio (L/D) of 4. The spinning dope was then degassed at 25 °C in a vacuum. The barrel was heated to 65−80 °C, and the curdlan or curdlan acetate filaments were spun using a lab-scale customised wet spinning unit (AIKI RIOTECH Co., Ltd., Aichi, Japan).[31] The filament was extruded through the spinneret, which was equipped with four types of inner metal meshes (30, 100, 200, and 300 meshes) to remove the undissolved substrate of more than 50 μm, which can lead to unstable spinning. After the fluid filament was passed through an air gap of 10 cm, it was coagulated in distilled water at room temperature (25 °C). The extrusion velocity (V_e) was set to 5.0 m min^{-1}, while the take-up velocity (V_t) of the godet roller was set to 25 m min^{-1}, thereby resulting in draw ratios (DR = V_t/V_e) of 5. The fibres were repeatedly washed off-line with hot water at 60 °C, and the water was changed at least four times over a total period of more than 5 days to thoroughly remove the residual [Emim][OAc]. The washed fibres were collected after air-drying for 1 day under constant tension.

Scheme 1. Experimental flow for preparation of curdlan acetate fibre and powder samples

Preparation of curdlan and curdlan acetate powders

After acetylation (or regeneration) of curdlan according to the procedures described above, a part of the reactant solution was appropriately diluted with DMSO and poured into methanol to precipitate white particles. The precipitate was filtered and washed with methanol and water repeatedly and freeze-dried for 2 days. The powder product was vacuum-dried at 70 °C until a constant weight was obtained and used for analysis of the chemical structure, solubility, and thermal properties.

Determination of the degree of substitution (DS)

The powder samples of curdlan and curdlan acetates were per-propionylated in a heterogeneous reaction system using trifluoroacetic acid anhydride (TFAA). TFAA (4 mL) and propionic acid (4 mL) were mixed at room temperature (25 °C) prior to the reaction. The vacuum-dried powder sample (100 mg) was added to the TFAA/propionic acid-mixed solution and heated at 50 °C until the suspended reaction solution became completely clear within 2−4 h. The resultant solution was poured into methanol (300 mL) while stirring to induce precipitation. The precipitate was filtered, washed with methanol, and dissolved in chloroform (6−10 mL). The resultant solution was re-precipitated in methanol/water (4:1, vol/vol), washed with methanol and water, and freeze-dried for 2 days. After vacuum-drying at 70 °C for 24 h, the DS of the Ac groups was determined by ^1H nuclear magnetic resonance (NMR) spectroscopy of the fully per-propionylated sample. Additionally, the distributions of Ac groups among the OH groups at C6-, C4-, and C2-positions of curdlan were estimated through ^{13}C NMR analysis of the pristine curdlan acetate powder.

The ^1H and ^{13}C NMR spectra were recorded in deuterated DMSO-d_6 or chloroform-d_1 using a JNM-ECA 600 spectrometer (JEOL Ltd., Tokyo, Japan). All NMR spectra were analysed using Delta NMR (JEOL Ltd., Tokyo, Japan), and the chemical shifts (δ, parts per million (ppm)) were referenced against tetramethylsilane (TMS, δ = 0 ppm) as the internal standard.

Polarised optical microscopy (POM) and birefringence measurements

An ECRIPSE E600 POM (Nikon Co., Tokyo, Japan) equipped with a DFC 450 charge-coupled device camera (Leica) was used to observe the orientation of the fibres. The polariser and depolariser were set at appropriate angles to obtain clear images. The average orientation of the amorphous and crystalline parts in each fibre sample was determined using the same POM equipped with a Berek compensator (Nichika Inc., Kyoto, Japan). The birefringence (Δn) of the fibres was calculated by dividing the retardation of the polarized light by the thickness of fibre, which was calculated from the linear density (titer) using the density of curdlan as 1.45 g cm^{-3}.[27] The total orientation factor (f_t) can be determined by dividing Δn by the maximum birefringence (Δn$_{max}$) of curdlan. However, the Δn$_{max}$ of curdlan has never been determined, and therefore, the value of Δn was regarded as the analogue factor for discussing the fibre orientation in this study.

Wide-angle X-ray diffraction

Two-dimensional (2-D) WAXD of the fibres was measured using a Micromax-007HF system (Rigaku Co., Tokyo, Japan) operating at a voltage of 40 kV and current of 30 mA with Cu Kα radiation (λ = 0.15418 nm) in the transmission geometry mode at room temperature and in a high-vacuum state. An imaging plate (BAS−SR 127, Fujifilm Co., Tokyo, Japan) and an imaging plate reader (RAXIA−Di, Rigaku Co., Tokyo, Japan) were used. The 2-D X-ray pattern analysis and conversion to a one-dimensional (1-D) X-ray pattern were performed using 2DP software (Rigaku Co., Tokyo, Japan). The degree of crystallite chain orientation (f_{cr}) was determined by an azimuthal scan of the meridional main interference taken from well-aligned fibres in the longitudinal direction. It is defined as (180°−WH)/180°, where WH represents the half width of the orientation peak from the intensity azimuthal profile.

Thermal analyses

Thermogravimetric analysis (TGA) was performed using a TGA-50 (Shimadzu Co., Kyoto, Japan) equipped with a gas flow controller (FC-60A, Shimadzu Co., Kyoto, Japan) and an analysis system (TA-60, Shimadzu Co., Kyoto, Japan). All samples were vacuum dried at 70 °C for 24 h prior to use, and the measurement temperature range was set from 50 to 500 °C at a heating rate of 10 °C min^{-1} in a N$_2$-flow rate of 50 mL min^{-1}. A sample (*ca.* 10 mg) was pre-dried at 120 °C for 2 h. The thermal decomposition temperature (T_d) was defined as the onset of a 5% weight loss ($T_{d-5\%}$).

The glass transition temperature (T_g) was investigated via dynamic mechanical analysis (DMA) using a DMA 8000 instrument (PerkinElmer Japan Co., Ltd., Yokohama, Japan) in a single cantilever mode. The powder samples (*ca.* 10 mg) were enclosed in a folded metal plate called "material pocket." The measurements were carried out under a N$_2$ atmosphere at a heating rate of 2 °C min^{-1} from 50 to 300 °C or to the temperature at which the T_g peak for each sample was clearly observed.

Water absorption test

Air-dried fibres with a length of 3.0 cm were immersed in distilled water for 24 h. The water-absorbed fibres were taken up from the water, gently wiped with paper to remove excess moisture on the surface, and immediately subjected to precise gravimetric measurements. The water absorbency of the fibre was evaluated based on the mass change before and after water absorption. The resultant fibre was regarded as a fibre in the wet state and used for the tensile test, as described below.

Mechanical properties

The linear densities (titre) of the fibres were determined by a precise gravimetric measurement of each air-dried fibre, which was cut to a length of 3.0 cm. Tensile tests were performed using an EZ test instrument (Shimadzu Co., Kyoto, Japan) with a tensile speed of 10 mm min^{-1} and an initial gauge length of 10 mm. The test was conducted more than five times for each fibre sample in the dry and wet states, and the average tensile strength was calculated.

Results and discussion

Synthesis and characterisation of curdlan acetate powders.
The acetylation of curdlan using [Emim][OAc] and a determined amount of IPAc was confirmed by Fourier-transform infrared (FT-IR) and ^{1}H NMR measurements (Figures S1 and S2), and no significant decrease in the molecular weight occurred during the reaction (Figure S3). Table 1 summarises the DSs of the powder-state products, IPAc amount, and its conversion ratio (conv.%). The DS increased from 0.09 to 1.58 as the IPAc amount increased, but the conv.% decreased from 94 to 53%, suggesting that a reaction time that is longer than 2 h is required at 80 °C to increase the conv.% and the resultant DS of curdlan acetate.

Figure 1a shows the entire ^{13}C NMR spectra of curdlan and curdlan acetate powders. Characteristic peaks of the curdlan skeleton were observed from 61 to 103 ppm. Furthermore, new peaks at approximately 170 and 21 ppm were detected in the spectra of curdlan acetates, which correspond to the carbonyl (C=O) and methyl (CH$_3$-) carbons of the Ac group, respectively. As shown in the expanded peaks attributed to the C=O carbons in Figure 1b, only one peak at 170.8 ppm was detected in the spectra of CdAc (0.1 and 0.2) suggesting that the Ac group was introduced to the OH group at the C6-position of curdlan.[32] Conversely, a small sharp peak at 170.6 ppm and a broad peak at approximately 169.7 ppm also appeared in the spectra of curdlan acetates with DSs exceeding 0.4, indicating that OH groups at not only C6- but also C2- and C4-positions were acetylated. The DSs of the C6-OH group and the sum of C2- and C4-OH groups, which were estimated using the integration ratio of the corresponding peaks, are presented in Table 1.

Curdlan acetates (DS = 0.1−1.0) were soluble in DMSO as well as the original curdlan, and ^{13}C NMR spectra were clearly obtained. However, the solubility of curdlan acetates with DSs

exceeding 1.3 became very poor despite heating at 80 °C. Other common solvents, such as water, acetone, and chloroform, did not dissolve curdlan acetates (DS = 1.3 and 1.5) (Figure S4), implying the difficulty in dry and wet spinning of these powders.

It was reported that acetylation of curdlan improves the thermal stability by preventing the fast dehydration associated with the OH groups. Precisely, curdlan triacetate (DS = 3) exhibited a 5% weight loss temperature ($T_{d-5\%}$) of 318 °C and 50% weight loss temperature of 361 °C,[33] which were higher than those of the original curdlan at 315 and 343 °C, respectively (Table S1). The precise DS, when high thermal stability as evaluated by $T_{d-5\%}$ is achieved, has not been clarified, but the TGA of curdlan acetate powders with different DSs (Figure S5a) implied that a DS of 0.8 was the boundary value, as shown in Figure 2. The peak-top temperature of differential TG (DTG$_{max}$) constantly increased from 343 to 381 °C as the DS of curdlan acetate increased, indicating that the thermal stability was improved by acetylation. Conversely, the $T_{d-5\%}$ of curdlan decreased once via regeneration and/or an extremely partial acetylation such as DS of 0.1 and 0.2. Then, it improved as DS increased, reaching a maximum value of 342 °C for curdlan acetate (DS = 1.0). A gradual decrease in the $T_{d-5\%}$ was observed as the DS further increased to 1.3 and 1.5; this decrease is expected to persist as the DS approaches the maximum DS value of 3, considering the relatively low $T_{d-5\%}$ (318 °C) of curdlan triacetate.[33]

DMA measurements of the curdlan acetate powders (Figure S5b) revealed that the glass transition temperature (T_g) of curdlan decreased from 280 to 206 °C with increasing DS from 0 to 1.5, as shown in Figure 2. Curdlan acetates (DS = 1.3 and 1.5) were found to have adequate heat-meltability (Figure S6), implying their applicability to melt spinning. However, curdlan acetates (DS ≤ 1.0) are not thermally processable, suggesting that the applicable moulding process is limited.

Table 1 Conversion rate of IPAc used for acetylation of curdlan in [Emim][OAc] (80 °C, 2 h) and the DS of curdlan (Cd) and curdlan acetate (CdAc) powders

Abbreviation	IPAc / eq./AGU	DS$_{Total}$ [a]	DS$_{C6-OH}$ [b]	DS$_{C2-/C4-OH}$ [b]	Conv. [c] / %
Cd (0)	—	0.00	N/A	N/A	—
CdAc (0.1)	0.1	0.09	0.09	N/A	94
CdAc (0.2)	0.25	0.23	0.23	N/A	93
CdAc (0.4)	0.5	0.45	0.39	0.06	90
CdAc (0.8)	1.0	0.75	0.41	0.34	75
CdAc (1.0)	1.5	1.06	0.56	0.50	71
CdAc (1.3) [d]	2.0	1.34	0.60	0.74	67
CdAc (1.5) [d]	3.0	1.58	0.43	1.15	53

[a,b] Determined by ^{1}H and ^{13}C NMR analyses of per-propionylated curdlan and curdlan acetate powders, measured in chloroform-d_1 containing 0.05 vol.% TMS. [c] Conversion ratio of IPAc, calculated from the measured DS, divided the theoretical DS estimated by the added amount of IPAc. [d] Not fabricated into the fibre owing to the poor spinnability of the dope.
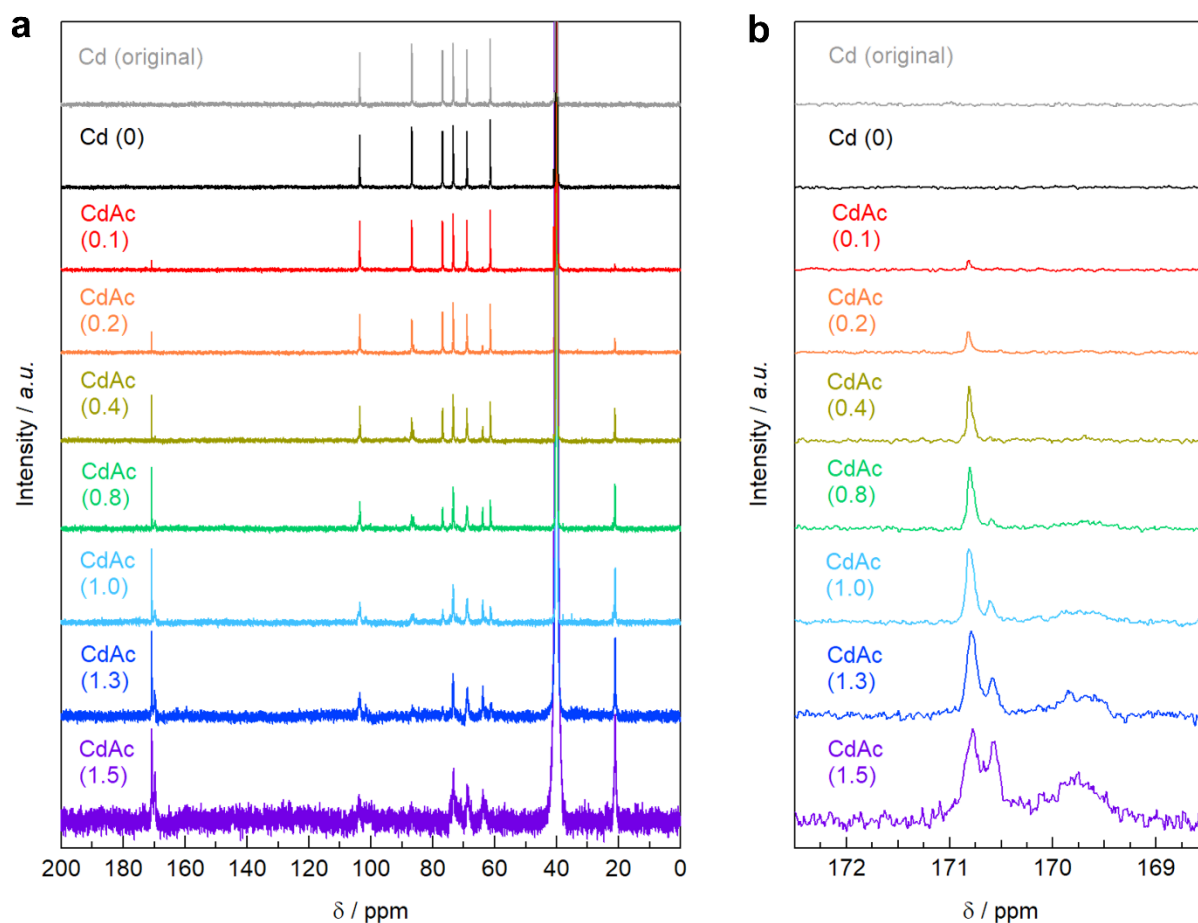
Figure 1. (a) ^{13}C NMR spectra of curdlan and curdlan acetate powders and (b) expanded spectra corresponding to carbonyl carbons of Ac groups, which were measured in DMSO-d_6 containing 0.05 vol.% TMS. The concentration of CdAc (1.3 and 1.5) solutions were very low owing to their insufficient solubility in DMSO (see Figure S4 in Supporting Information), and therefore, the spectra obtained with low intensity were significantly expanded compared to others and are displayed above.
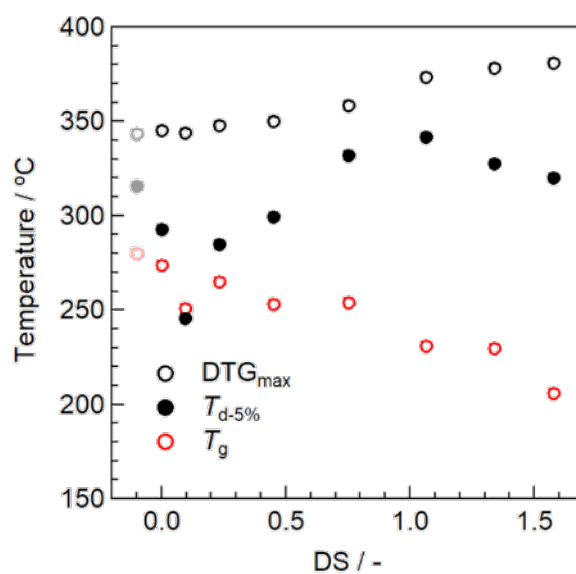
Figure 2. DTG$_{max}$, $T_{d-5\%}$, and T_g of the original and regenerated curdlan powders and curdlan acetate powders as a function of the DS, which were measured by TGA and DMA.

Morphology and structural analyses of curdlan acetate fibres with low DS.

Curdlan and curdlan acetates with low DSs (0–1.0) are not applicable to thermal moulding, and their fabrication into fibres was realised via a continuous process of synthesis and wet spinning utilising [Emim][OAc] as an acetylation medium and spinning solvent. As shown in the optical micrograph in Figure 3a, uniform fibres with linear density (titre) of 5.4–6.6 tex were obtained, and their molecular chain orientation along the fibre axis was observed by polarized microscopy (POM, Figure S7).

Although there seemed to be cavity-like dots in the optical micrographs of fibres with increasing DS, SEM observation indicated that the inner and outer structures of curdlan acetate (DS = 0.8) fibre were dense and smooth (Figure S8) as well as the regenerated curdlan fibre.[31] Based on the decrease in the solubility of curdlan acetates in [Emim][OAc] with increasing DS (Figure S4), the dots observed by optical microscopy could be precipitates with diameters below 50 μm from the dope (and/or localised crystallites of the curdlan acetate), which were passed through the inner mesh of the spinning barrel and unexpectedly embedded into the fibres. When the DS of curdlan acetate exceeded 1.3, the originally clear reaction solution became cloudy because of the precipitation of the products and changed into an elastic gel-like state after the reaction. The resultant mixture was not wet-spun because of the loss of the spinnability of the dope, that is, appropriate viscoelasticity. Such technical limitations in wet spinning, caused by the change in the solubility of curdlan acetate and spinnability of the dope, might be improved by optimising the spinning conditions, for example, substrate concentration or spinning temperature.

The change in solubility of curdlan acetate as DS increased can be caused by a change in the crystallinity. As shown by the 2-D X-ray fibre diagrams in Figure 3a, the regenerated curdlan fibre showed three reflections corresponding to the (100), (110), and (203) planes, respectively, which belong to a typical hydrate crystalline form composed of a triple-helical molecular chains. [28, 31] Similar diffraction patterns were observed until the DS of the curdlan acetate fibres reached 0.4, although the reflections on the equator of the first layer line changed from ark to ring shapes, which is related to the decrease in the degree of crystalline orientation (f_c) from 72% to 68%. In contrast, curdlan acetate fibres (DS = 0.8 and 1.0) showed apparently different 2-D X-ray fibre diagrams and a high f_c of 83−86%. In their 1-D diffraction pattern (Figure 3b), the broad peak of the regenerated curdlan fibre at approximately 20° was sharpened, due to the decrease in hydrated water by acetylation. Additionally, the other peak at 6.2° shifted to 6.9°, implying a change in the crystalline form itself.
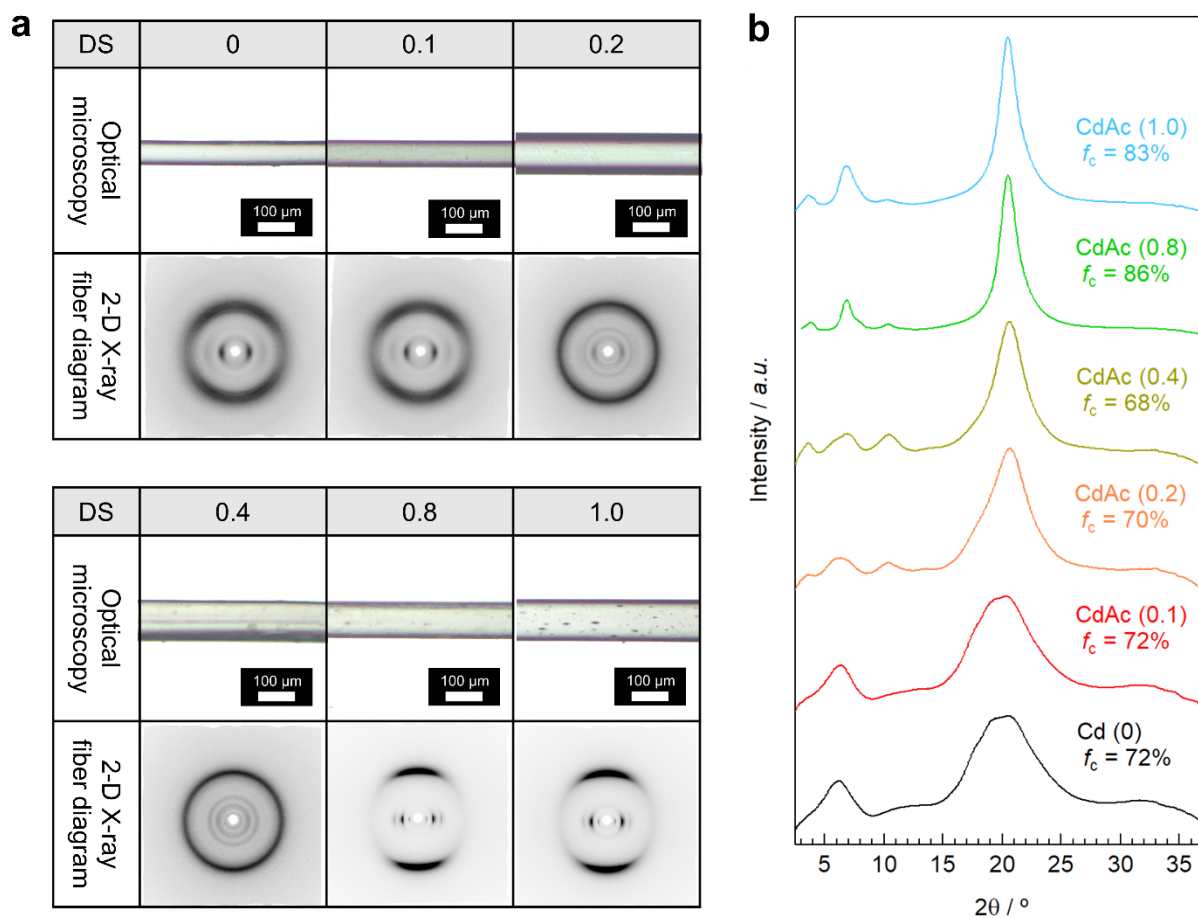
Figure 3. (a) Optical microscopy images and 2-D X-ray fibre diagrams and (b) 1-D X-ray diffraction patterns and the degree of crystalline chain orientation (fc) of regenerated curdlan fibre and curdlan acetate fibres with DS of 0.1–1.0.

The triple helical structure of curdlan is stabilised by hydrogen bonding via the C2-OH group.[29] Until the DS of curdlan acetate exceeded 0.4, only the C6-OH group was acetylated (Figure 1); therefore, the original crystallinity did not change considerably, although the crystalline orientation was slightly inhibited. In contrast, an adequate amount of the C2-OH group (and C4-OH group) was also acetylated when the DS exceeded 0.8 (Table 1). Then, the triple helical structure could not be retained, which may induce a significant change in the crystalline structure. However, the resultant diffraction patterns (Figure 3a,b) are distinctly different from that of curdlan triacetate with a single helical structure.[34] A detailed structural analysis of the improved fibre sample with high crystallinity and orientation is required to elucidate the unique structure of the moderately acetylated curdlan fibres.

**Correlation between DS and mechanical properties of curdlan acetate fibres.**

Figure 4a shows the stress-strain (S-S) curves of curdlan and curdlan acetate fibres in the dry state. Similar to our previous report,[31] the regenerated curdlan fibre showed high ductility owing to its triple helical structure. Although the tensile strength decreased as DS increased from 0.1 to 0.2, the high elongation at break remained over 30%. Conversely, the shape of the S-S curves clearly changed at DSs exceeding 0.4, with a decrease in the elongation of less than 10%, which might be caused by the change in the crystalline structure (Figure 3).

The average values of the tensile strength and Young's modulus are summarised in Figure 4b with the Δn value, which represents the total orientation in both the amorphous and crystalline parts. The Δn of the curdlan acetate fibres tended to increase with increasing DS, and the amorphous orientation was considered to improve dominantly, based on the slight decrease in f_c (Figure 3b). In general, the improved molecular chain orientation correlates with enhanced tenacity, and the contribution of the orientation in the amorphous part is larger than that in the crystalline part in the case of polysaccharide-based fibres.[25] However, the tensile strength of curdlan acetate fibres consistently decreased with increasing DS, implying that the mechanical strength depended on the crystalline structure more than the amorphous orientation.

The decrease in the tensile property with acetylation is a phenomenon similar to that of cellulose,[10, 11] mainly because of the lowering of the hydrogen bonds. Kosan et al. reported that the tenacity of the cellulose acetate fibres with DS of 0−2.38 significantly decreased from 57 to 11 cN tex^{-1} although the elongation remained the same as 10%.[11] In the case of curdlan acetate fibres, the degree of the decrease in the tensile strength was relatively small. However, the significant decrease in elongation was considered to be a unique tendency of curdlan acetate, where the crystalline structure can change from a triple helix (DS = 0) to a single helix upon acetylation (DS = 3).[33]

Notably, Young's modulus of curdlan acetate certainly increased at a DS of 0.4, although those of cellulose acetate consistently decreased as the DS increased.[10] This improvement may correlate with an increase in the crystalline elastic modulus, such as the change in the pitch of the helices forming the crystalline structure.[35] However, the tensile strength and Young's modulus gradually decreased with a further increase in the DS. This embrittlement with partial acetylation can be attributed to the crystallinity and incorporation of fine particles that precipitated from the [Emim][OAc] dope with decreasing solubility. Therefore, the preparation of the enhanced curdlan acetate fibres without impurities is our future task; this technical advancement is essential for the accurate analysis of the crystalline elastic modulus.
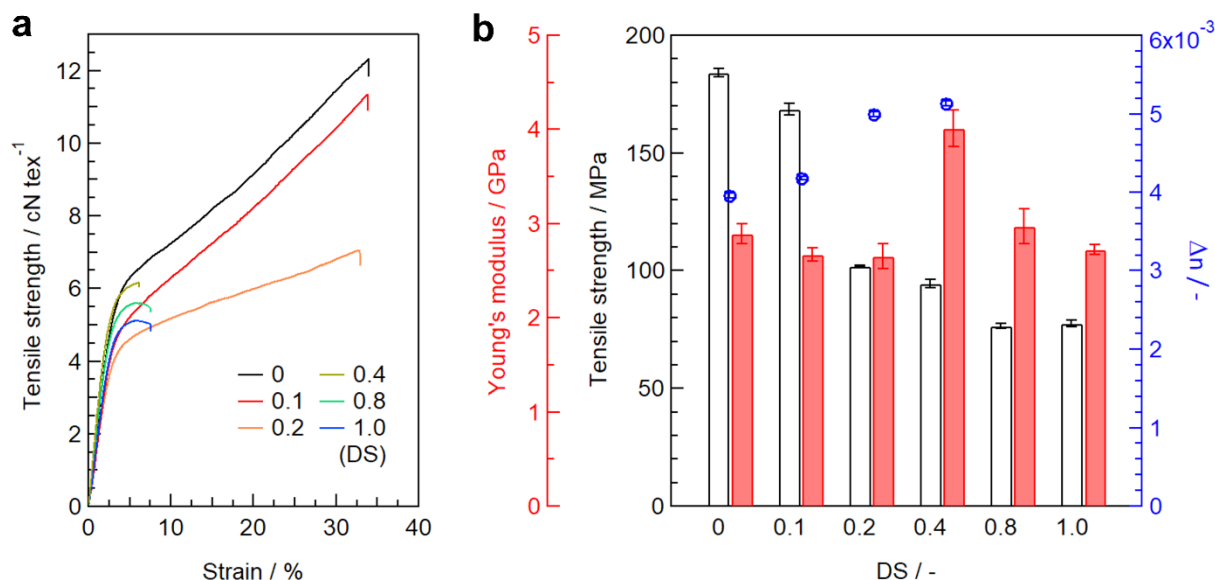
Figure 4. (a) Stress−strain curves and (b) average tensile strengths, Young's moduli, and the Δn values of the regenerated curdlan fibre and curdlan acetate fibres as a function of DS.

Among a wide variety of polysaccharides, curdlan has unique properties such as high water absorbency in addition to its excellent ductility,[27, 31] and the regenerated curdlan fibre prepared in this study also showed high water absorption ability of 85 wt.%. However, the excess absorption of water is predicted to cause a significant loss of mechanical strength, which may limit its application range. The water absorbency of curdlan is attributed to the incorporation of water molecules into its intermolecular and intramolecular chains via the ether oxygen in the glucopyranose ring and the C4-OH group.[28] Therefore, the water absorption ability can be suppressed by substituting the C4-OH group with the Ac group. As expected, the water absorption test of curdlan acetate (DS = 0.8) fibre, in which a certain amount of Ac group was introduced to the C4-OH group, demonstrated an effective suppression of the water absorbency to 15 wt.% (Table S2).

The tensile tests of the fibres in the dry and wet states (Figure S9) revealed that the tenacity of the regenerated curdlan fibre decreased from 12.6 cN tex^{-1} (dry) to 0.34 cN tex^{-1} (wet), corresponding to an extremely small wet-to-dry tenacity ratio of 0.03. In contrast, the tenacity of the curdlan acetate (DS = 0.8) fibre in the dry and wet states were 5.5 cN tex^{-1} and 2.8 cN tex^{-1}, respectively. Therefore, the wet-to-dry tenacity ratio successfully improved to 0.5 by appropriately suppressing the water absorption. Asaadi et al. reported that the wet-to-dry tenacity ratio of the regenerated cellulose fibre decreased from 0.93 to 0.61 by acetylation (DS = 0.75),[10] because the molecular alignment in the crystalline part was disrupted with trace amounts of the introduced Ac group, and water was then absorbed in the resultant amorphous part. These different trends in the wet tenacity of curdlan acetate and cellulose acetate fibres suggest that the improvement of the wet-to-dry tenacity ratio of polysaccharide-based fibres cannot be simply realised by hydrophobisation, such as acetylation, and therefore, depends on the original and resultant crystalline structures. Referring to the high wet-to-dry tenacity ratio of the regenerated cellulose fibres (ca. 0.6–1.0),[25] that of curdlan acetate fibre should be improved, and the physical and mechanical properties can be tuned by precise control of the DS and type of the introduced functional groups.

As demonstrated above, the continuous process of partial acetylation of curdlan and subsequent wet spinning enabled the preparation of curdlan acetate fibres with DSs less than 1.0, thereby exhibiting new potential for curdlan as a mouldable and functional material without sacrificing its inherent biodegradability [37] for a variety of applications. This process was realised under simple operation and mild conditions using only [Emim][OAc], a minimal amount of IPAc, and water. The recyclability of the [Emim][OAc] and the scalability of the acetylation reaction have already been demonstrated in previous reports.[21, 36] Although our process is still a suboptimal setup utilising a small monofilament system and therefore requires a detailed optimisation of the reaction and spinning conditions, it can be an environmentally and economically friendly process that is applicable to various types of polysaccharides and ester groups.

Conclusions

Curdlan acetate fibres with low DSs ranging from 0.1–1.0 were successfully prepared via a continuous process of chemical modification of curdlan and wet spinning using an ionic liquid, [Emim][OAc], as the catalyst and dual solvent. Acetylation of curdlan using IPAc proceeded only on the C6-OH group at extremely low DSs of 0.1 and 0.2, while the C2- and C4-OH groups were also acetylated at DSs exceeding 0.4. The partial acetylation of curdlan improved the $T_{d-5\%}$ from 293 °C to 342 °C, and curdlan acetates were found to acquire thermal processability when the DS exceeded 1.0. Originally, the regenerated curdlan fibre was ductile in both dry and wet states: the elongation at break was 34% and 130%, respectively, which was attributed to its triple helical crystalline structure. Additionally, it had an exceptionally high water absorbency of 85 wt.%, thereby causing a significant decrease in tensile strength in the wet state. In contrast, the curdlan acetate fibres became stiff, and the wet-to-dry tenacity ratio significantly increased from 0.03 to 0.5 by suppressed water absorbency (cf. 15 wt.% at DS = 0.8) owing to the moderate substitution of C4-OH group (which contributes to the incorporation of water into the curdlan molecules). Such improvements in fibre properties were correlated to the change in the crystalline structure by acetylation of the C2-OH group (which stabilises the original triple helical structure). The demonstrated continuous process for fabricating curdlan acetates with low DSs can be a way of solving a conventional problem in the utilisation of insoluble and non-thermal meltable polysaccharides, namely, a trade-off between acylation to improve their mouldability and the loss of the inherent biodegradability. Further, this process can be a versatile with respect to the types of substrate polysaccharides and ester donors, and is an environmentally and eco-friendly process using safe and non-corrosive reagents, simple operations, and mild conditions. The proposed technique and obtained insights on the relationship between the fibre properties and structure through this study will create new possibilities for various applications of polysaccharides as biodegradable and functional materials.

Supporting information

The following files are available free of charge:

ATR-mode FT-IR and ^{1}H NMR spectra, GPC chromatograms, the weight-average molecular weight (M_w), polydispersity, solubility in DMSO, water, and [Emim][OAc], TG and DMA curves, summary of thermal properties, pictures of hot-pressed films, linear density (titre), POM and SEM images, Δn values, water absorbency, S-S curves and average tensile properties (dry and wet) of regenerated curdlan fibre and curdlan acetate fibres with different DSs are shown in PDF.

Funding

Acknowledgements

Conflicts of interest

The authors declare no competing financial interest.

References

1. D. Griggs, M. Stafford-Smith, O. Gaffney, J. Rockström, M. C. Öhman, P. Shyamsundar, W. Steffen, G. Glaser, N. Kanie and I. Noble, *Nature*, 2013, **495**, 305-307.

2. N.-I. S. Abdul-Latif, M. Y. Ong, S. Nomanbhay, B. Salman and P. L. Show, *Bioengineered*, 2020, **11**, 154-164.

3. R. Thompson, C. Moore, A. Andrady, M. Gregory, H. Takada and S. Weisberg, *Science*, 2005, **310**, 1117-1117.

4. V. Goel, P. Luthra, G. S. Kapur and S. S. V. Ramakumar, *Journal of Polymers and the Environment*, 2021, **29**, 3079-3104.

5. P. Nechita and M. Roman *Coatings*, 2020, **10**, 566.

6. P. Cazón, G. Velazquez, J. A. Ramírez and M. Vázquez, *Food Hydrocolloids*, 2017, **68**, 136-148.

7. S. Puanglek, S. Kimura and T. Iwata, *Carbohydrate Polymers*, 2017, **169**, 245-254.

8. W. Zhai and T. Iwata, *Polymer Degradation and Stability*, 2019, **161**, 50-56.

9. K. Kamide and M. Saito, *European Polymer Journal*, 1984, **20**, 903-914.

10. S. Asaadi, T. Kakko, A. W. T. King, I. Kilpeläinen, M. Hummel and H. Sixta, *ACS Sustainable Chemistry & Engineering*, 2018, **6**, 9418-9426.

11. B. Kosan, S. Dorn, F. Meister and T. Heinze, *Macromolecular Materials and Engineering*, 2010, **295**, 676-681.

12. C. M. Buchanan, R. M. Gardner and R. J. Komarek, *Journal of Applied Polymer Science*, 1993, **47**, 1709-1719.

13. R. J. Komarek, R. M. Gardner, C. M. Buchanan and S. Gedon, *Journal of Applied Polymer Science*, 1993, **50**, 1739-1746.

14. C. J. Rivard, W. S. Adney, M. E. Himmel, D. J. Mitchell, T. B. Vinzant, K. Grohmann, L. Moens and H. Chum, *Applied Biochemistry and Biotechnology*, 1992, **34**, 725-736.

15. R. P. Swatloski, S. K. Spear, J. D. Holbrey and R. D. Rogers, *Journal of the American Chemical Society*, 2002, **124**, 4974-4975.

16. W. Bai, F. Shah, Q. Wang and H. Liu, *International Journal of Biological Macromolecules*, 2019, **130**, 922-927.

17. R. Kakuchi, M. Yamaguchi, T. Endo, Y. Shibata, K. Ninomiya, T. Ikai, K. Maeda and K. Takahashi, *RSC Advances*, 2015, **5**, 72071-72074.

18. T. Kakko, A. W. T. King and I. Kilpeläinen, *Cellulose*, 2017, **24**, 5341-5354.

19. H. Hanabusa, E. I. Izgorodina, S. Suzuki, Y. Takeoka, M. Rikukawa and M. Yoshizawa-Fujita, *Green Chemistry*, 2018, **20**, 1412-1422.

20. M. Gericke, P. Fardim and T. Heinze, *Molecules*, 2012, **17**, 7458-7502.

21. Q. Van Nguyen, S. Nomura, R. Hoshino, K. Ninomiya, K. Takada, R. Kakuchi and K. Takahashi, *Polymer Journal*, 2017, **49**, 783-787.

22. S. Elsayed, S. Hellsten, C. Guizani, J. Witos, M. Rissanen, A. H. Rantamäki, P. Varis, S. K. Wiedmer and H. Sixta, *ACS Sustainable Chemistry & Engineering*, 2020, **8**, 14217-14227.

23. L. K. J. Hauru, M. Hummel, A. Michud and H. Sixta, *Cellulose*, 2014, **21**, 4471-4481.

24. J. Zhang, J. Wu, J. Yu, X. Zhang, J. He and J. Zhang, *Materials Chemistry Frontiers*, 2017, **1**, 1273-1290.

25. H. Sixta, A. Michud, L. Hauru, S. Asaadi, Y. Ma, A. W. T. King, I. Kilpeläinen and M. Hummel, *Nordic Pulp & Paper Research Journal*, 2015, **30**, 43-57.

26. R. Zhang and K. J. Edgar, *Biomacromolecules*, 2014, **15**, 1079-1096.

27. R. H. Marchessault, Y. Deslandes, K. Ogawa and P. R. Sundararajan, *Canadian Journal of Chemistry*, 1977, **55**, 300-303.

28. C. T. Chuah, A. Sarko, Y. Deslandes and R. H. Marchessault, *Macromolecules*, 1983, **16**, 1375-1382.

29. G. Fittolani, P. H. Seeberger and M. Delbianco, *Peptide Science*, 2020, **112**, e24124.

30. T. Harada, A. Misaki and H. Saito, *Archives of Biochemistry and Biophysics*, 1968, **124**, 292-298.

31. S. Suzuki, A. Togo, H. Gan, S. Kimura and T. Iwata, *ACS Sustainable Chemistry & Engineering*, 2021, **9**, 4247-4255.

32. C.-Y. Chien, Y. Enomoto-Rogers, A. Takemura and T. Iwata, *Carbohydrate Polymers*, 2017, **155**, 440-447.

33. H. Marubayashi, K. Yukinaka, Y. Enomoto-Rogers, A. Takemura and T. Iwata, *Carbohydrate Polymers*, 2014, **103**, 427-433.

34. K. Okuyama, Y. Obata, K. Noguchi, T. Kusaba, Y. Ito and S. Ohno, *Biopolymers*, 1996, **38**, 557-566.

35. H. Gan, T. Kabe, S. Kimura, T. Hikima, M. Takata and T. Iwata, *Polymer*, 2019, **172**, 7-12.

36. R. Milotskyi, L. Szabó, T. Fujie, K. Sakata, N. Wada and K. Takahashi, *Carbohydrate Polymers*, 2021, **256**, 117560.

37. J. Seok, Y. Enomoto and T. Iwata, *Polymer Degradation and Stability*, 2022, **197**, 109855.